5-2023

Investigating the role of CNAG_05113 in the carnitine biosynthesis pathway in *Cryptococcus neoformans.*

Jasmine Meltzer

Rodrigo Catalan-Hurtado

Perry Kezh

Kerry Smith

Investigating the role of CNAG_05113 in the carnitine biosynthesis pathway in *Cryptococcus neoformans*.

Jasmine Meltzer*, Rodrigo Catalan-Hurtado, Perry Kezh, and Kerry Smith

Department of Genetics and Biochemistry and
Eukaryotic Pathogens Innovations Center,
Clemson University, Clemson, SC, 29634

Abstract

Cryptococcus neoformans, the leading cause of fungal meningitis, is a fungal pathogen that causes severe infection of the central nervous system in patients with compromised immune systems, typically caused by HIV/AIDS. *C. neoformans* infections are present in developed countries including the United States, but most fatalities occur in sub-Saharan Africa where antiretroviral therapy, the treatment for HIV/AIDS, is less accessible. Current treatments for severe cryptococcal infections are extensive and outdated. There is a critical need for an improved understanding of the fungus and new targeted therapies. Our goal is to identify metabolic pathways important to the survival of *C. neoformans* in the human host that can then be targeted for the development of new antifungal reagents. Lung alveolar macrophages, which present a first line of host defense against *C. neoformans* infection, provide a glucose- and amino acid-poor environment, and nonpreferred carbon sources such as lactate and acetate are likely important early in establishment of a pulmonary infection. Utilizing a genetic screen performed by a graduated PhD student in my lab to identify genes necessary for growth on acetate, we have discovered that the last step of carnitine biosynthesis is required. Our goal was to identify other steps of the carnitine biosynthetic pathway. Using the amino acid sequence of the fungal *Candida albicans* 4-trimethylaminobutyraldehyde dehydrogenase (TMABADH), the third enzyme of the carnitine biosynthesis pathway which converts 4-trimethylaminobutyraldehyde (TMABA) to gamma-butyrobetaine (γBB), we identified CNAG_05113 as the encoding gene in *C. neoformans*. Using a strain in which the CNAG_05113 gene was deleted, the mutant was tested for growth and virulence deficiencies. CNAG_05113 cells have inhibited growth in conditions with acetate as the sole carbon source. When reintroduced to carnitine and carnitine pathway intermediates, growth of mutant cells was restored. These results indicate that CNAG_05113 encodes the third step in carnitine biosynthesis. Future research is to identify the genes encoding other steps of the carnitine biosynthesis pathway and to biochemically characterize the encoded enzymes.

Introduction and Literature Review

Cryptococcus neoformans is a fungal pathogen that causes severe infection of the nervous system in patients with compromised immune systems, typically caused by HIV/AIDS. Recognized as a major health threat in the 80's during the AIDS epidemic, Cryptococcal meningitis is responsible for more than 100,000 HIV related deaths each year[1]. Cryptococcal infection is primarily found in sub-Saharan Africa where HIV diagnosis is prevalent and HIV treatments, such as antiretroviral therapies, are less accessible. Current treatments for severe cryptococcal infection are intensive and outdated. There is a critical need for an improved understanding of the fungus and new targeted therapies to combat one of the leading causes of death from HIV/AIDS, where cryptococcal meningitis is thought to be responsible for more annual deaths than tuberculosis[2].

Cryptococcus neoformans is a phylum Basidiomycota fungus that is ubiquitous to our natural environment. It is distinguished from other disease-causing yeast, such as *Candida albicans*, by capsule and melanin virulence factors[3]. *C. neoformans* is distinguished from its close relative, *C. gattii*, by prevalence of infection in AIDS patients[3]. Both species have multiple genetically diverse subgroups which differ geographically with disease incidence. Research about cryptococcosis, diseases caused by *Cryptococcus*, developed rapidly during the early 1980's when AIDS began spreading as it is a major risk factor for development of disease.

Cryptococcus infections are primarily spread through avian excretion and decaying tree material[4]. A typical incidence of infection occurs when fungal cells are inhaled from environmental sources. Cells are quickly cleared by immunocompetent hosts, but in individuals with compromised immune systems due to HIV, *C. neoformans* can develop pneumonia which spreads to the meninges. Fatal infection occurs when cells pass the blood brain barrier and acute meningitis develops, where intracranial pressure rises causing brain swelling, congestion, and hemorrhaging. This can manifest in physical symptoms such as headache, hearing or vision loss, malaise, and stroke[5]. Diagnosis is best performed through antigen detection in cerebrospinal fluid, or culturing cells from biopsy. Delayed diagnosis due to contrasting symptoms is a common cause of unexpected death in patients.

Cryptococcal infection is most prevalent in Africa, directly related to HIV infection in the region which carries more than 70% of global HIV infections[6]. Infection is primarily found in Nigeria, Ethiopia, and Uganda, correlating with HIV incidence[4], in addition to South America, Southeast Asia- especially Thailand, and some populations of Europe, particularly the United Kingdom[4]. There is a considerable amount of global heterogeneity across these populations of fungal structure which contributes to infection.

Cryptococcus is thought to be in spore form to infect the host as growing cells are too big to penetrate the alveolar tissue. Basidiospores are often smaller than 4 μm in yeast form but can also infect hosts as sexual spores. Encapsulated fungal cells can survive in the host after respiratory

inhalation. Basidiospores are opportunistic and are more susceptible to infect a t-cell immunodeficient host[7]. Pathogenesis of *Cryptococcus* is exacerbated by the capsule and melanin virulence factors. Polysaccharide capsule provides host defenses as it is difficult to phagocytize and reduces host immune response when present. Melanin increases host survival by acting as an antioxidant and inhibiting host antibodies. Mannitol is also often produced by *Cryptococcus* cells, which allows for heat resistance and resistance to osmotic stress[7].

Additionally, carbon source usage is important for virulence as nutrient availability can influence fitness in the host. Carbon and nitrogen are typically the primary energy sources for biosynthetic activity in *Cryptococcus*, and large quantities are needed from the environment. In vivo, the main carbon sources used by *Cryptococcus* are glucose, lactate, and acetate[8]. While glucose is the primary source of carbon in cells, acetate is used as a primary carbon source in cells in the host when glucose availability is low[9].

In order to properly metabolize carbon in vivo, fungal cells need carnitine. The carnitine biosynthetic pathway has been successfully characterized in the fungal pathogen *Candida albicans*; however, its role in virulence has not been reported. Carnitine is an essential metabolite responsible for the intracellular transport of long chain fatty acids and acetyl units into the mitochondria during carbon metabolism. Other carnitine functions include energy storage, excretion of toxic acyl units, and regulating acyl-CoA content in the cell. Mammals can obtain carnitine through diet and synthesize it, and this pathway has been characterized first in rats, then *Neurospora* and *Candida*. Likely, the pathway in *Cryptococcus* is similar to that of *Candida*. *Candida* creates carnitine de novo through a complex biochemical pathway. Starting with trimethylated amino acid lysine (TML), Candida catalyzes TML with TML dioxygenase (TMLD) to form 3-hydroxy-TML (HTML). HTML is then catalyzed by pyridoxal 5'-phosphate PLP-dependent aldolase (HTMLA) to form 4-trimethyl amino butyraldehyde (TMABA). TMABA dehydrogenase catalyzes the reaction of TMABA to form y-butyrobetaine (γBB) which forms L-carnitine catalyzed by the enzyme y-BB dioxygenase (BBD)[10] (**Figure 1**). This pathway was discovered by Strijbis *et al.*, where the lab created Candida mutants deficient in the four enzymes of the pathway. These mutants were unable to use fatty acids and/or acetate as a sole carbon source. Mutants only had restored growth if pathway intermediates were reintroduced that were involved in later steps of the pathway to the enzyme[9].

Current treatments for *Cryptococcus* are outdated and have poor outcomes in patients. 35-40% of individuals diagnosed with cryptococcal meningoencephalitis die within three months[4]. Current drugs are decades old and include three antifungal agents: polyenes such as amphotericin B, azoles such as fluconazole, and pyrimidine analogue flucytosine also known as 5-FC. Amphotericin is the main treatment, which functions by binding to the cell wall and inducing death. When combined with 5-FC, the highest fungal clearance rate is shown. This is the typical treatment plan in high resource countries, however impoverished countries with higher prevalence of

cryptococcal infection have difficulty administering these drugs intravenously. Often, these poorer countries use oral fluconazole and oral 5-FC combination therapy which is a less effective treatment method. Additionally, resistance to all three drug groups has been observed in these antifungal classes. For these reasons, there is an urgent need for new drugs to treat cryptococcal meningitis that target virulence factors or other vital components to cell survival.

The goal of this project is to research possible new therapeutic targets to replace these outdated current treatments which are easily accessible in developing countries which need it most. We have hypothesized that the carnitine pathway is a potential target for therapeutic agents to kill fungal cells. The lab has obtained multiple *Cryptococcus* mutants deficient in genes of unknown function from an external team. Through acetate screening, the CNAG_05113 mutant, called ALD13 in the lab, was identified as having deficient growth on acetate in normal conditions. Based on DeepMito location and sequence analysis, our lab has hypothesized that this mutant is missing a vital gene for the synthesis of the enzyme involved in the third step of the carnitine biosynthesis pathway, TMABA dehydrogenase. To test this hypothesis, we will perform carnitine and γBB rescue to reintroduce intermediates in the pathway that are found after TMABA dehydrogenase. We predict that the reintroduction of carnitine and γBB should restore normal cell growth on acetate. Unfortunately, TMABA is not readily available on the market or else a TMABA rescue experiment would support our hypothesis further. Once we determine the function of the deficient gene in our mutant, we can potentially target it for therapeutic use.

Methods

Spot Assay for Phenotype

C. neoformans cells were grown on 1x YNB + 2% carbon source agar plates to assess phenotype in different environments. Wild type K99 strain was used as a control to compare to the ALD13 mutant strain. Cells were cultured overnight, and then refreshed in the morning for a three-hour subculture. Cell concentration was counted using the hemocytometer under microscope to ensure an equal number of cells in experimentation. Cells were then isolated from the media through centrifugation and washed twice with PBS. Cells were resuspended in PBS and a serial dilution was performed to a three-fold final concentration of 10^3. Cells were then plated in 2 uL spots on both glucose and acetate agar plates. Plates were then incubated for 48-72 hours at either 30°C and 37°C.

Growth Curve Preparation

A common growth curve protocol was used to prepare 96 well plates for reading using either the Log Phase plate reader, or the Gen5 plate reader. First, cells were grown overnight and refreshed in the morning in a 3-hour subculture. Cells of the subculture were counted using the hemocytometer, and then enough cells to make a 1000 cells/uL solution were extracted and spun down. Cells were washed with PBS and resuspended with media. Media was specific to the conditions of each variable in the experiment- a 2% A and 2% G media was created and used to resuspend for acetate and glucose experiments. This media contained a 1X YNB, 2% carbon source (glucose or acetate), and ddH_2O to dilute. Cells were then plated with variable amounts of media to vary cell concentration and incubated in a 30°C shaker to be read for analysis over a 72-hour period.

Testing the Best Concentration for Growth Curve

Prior to the first carnitine rescue experiment, the best concentration of cells to use for the experiment needed to be determined. To do this, the growth curve preparation protocol was followed with both 2% A and 2% G media. Cells were then plated in 96 well plate at 5 different concentrations: a 1000X solution containing 200 uL of the 1000 cells/uL solution and no extra media, a 750X solution containing 150 uL of the 1000 cells/uL solution with 50 uL of extra media per well, and so on for 500X (500 cells/uL) concentration, 250X concentration, and a 25X concentration. Cells were then incubated at 30°C and using the Gen5 microplate reader software, 24-, 48-, and 72-hour timestamps were taken for analysis.

Growth Curves with Biotek LogPhase Continuous Microplate Reader

The LogPhase machine generates a consistent growth curve as it takes automatic timestamps once activated every 5 minutes for 72 hours at 37℃ at 600 nm OD. After following the growth curve protocol, cells were plated at a 250X concentration of 250 cells/uL with each well containing 150 uL of appropriate media and 50 uL of the 1000 cells/uL solution. For the first experiment, only 1 plate was used to test the wildtype K99 growth vs the ALD13 mutant growth in 2%A media, 2%A + 2mM concentration of carnitine, and 2%A + 200 uM concentration of carnitine. Each condition contained four well replicates (**Figure 2).**

Data was then exported and analyzed using excel to compute a trendline, which averaged the four well replicates of each condition.

This experiment was also replicated with the BBOX (CNAG_00403) mutant, which has been shown by other lab members to have no growth on acetate without carnitine addition. This was to provide a negative control for this experiment based on previously found results. This experiment was done with both 2%A and 2%G media, with the addition of carnitine as an experimental group (**Figure 3).**

Gamma-Butyrobetaine and Carnitine Spot Assay Rescue

Spot assay was performed to analyze phenotype with addition of carnitine and γBB to agar plate media. A 2 mM carnitine concentration was added to a standard 2% A plate recipe, and 2%A + 200 uM gBB plates were also used to test γBB rescue. A 3X serial dilution was performed and spotted onto plates in 2 uL spots. Each plate contained both K99 cells and ALD13 mutant cells to compare results. Plates were incubated at 30°C and 37°C in double replicates (**Figure 4).**

Growth Curves with Gen5 Microplate Reading Software- 600 nm Absorbance Optical Density

After the standard growth curve protocol referenced above was performed, 96 well plates were incubated in the 30℃ shaker and time stamps were taken in 24-hour increments using the Gen5 Microplate Reader machine (24, 48, and 72 hr). This experiment was performed to test carnitine and γBB rescue, using media containing a carbon source and 1X γBB + 2 mM carnitine or 200 uM γBB concentrations. Both 2%A and 2%G were used as carbon sources.

Melanin Spot Assay

Standard spot assay protocol performed on K99 wild type cells and ALD13 mutant cells on melanin plates. Plate recipe is agar with 8 mg/mL KH_2PO_4, 2 mg/mL glucose, 2 mg/mL L-glycine, 1 µg/mL $_D$-biotin (H/B7), 1µg/mL thiamine, 0.92 mg/mL $MgSO_4$, and 0.4 mg/mL $_L$-3,4-

dihydroxyphenylalanine. Plates were incubated in both 30°C and 37°C for 48-72 hours and then imaged.

Capsule

Wild type and ALD13 cells were cultured overnight. 100 uL of overnight culture was washed with PBS and resuspended in a DMEM + 10% fetal bovine serum media. Cells were then plated in 500 uL spots with 500 uL more of media and cultured in the 37°C + 5% CO_2 incubator for 4 days at 37°C. After incubation, cells were extracted and resuspended in PBS. 3 uL India ink + 7 uL culture + PBS were plated on microscopic slides and imaged using the Leica stellaris confocal microscope (**Figure 5).**

T-Test and Bar Chart Data Analysis

Performed a T-test data analysis on growth curve data. Compiled data from two unique growth curve experiments of wild type and mutant compared to rescue with carnitine or γBB with the purpose to determine the variance in our data and how representative our mean values are in bar charts. Then the average of the 48-hour timestamp of the unique growth curve experiments was plotted for both carnitine and γBB rescue in acetate and glucose. Standard error was added to the bar charts to analyze accuracy of data.

Results and Discussion

Overall, experimental results were consistent with our hypothesis. A clear growth defect of the ALD13 mutant was observable on acetate compared to glucose at both 30 °C and 37 °C (**Figure 6, Figure 7)**. This indicates that the missing genes in ALD13 are involved in acetate metabolism, which is further supported by the DeepMito biocomputing method location prediction of the CNAG_05113 protein to be localized to the mitochondrial inner membrane[12]. There was also homology found with both the human and candida TMABADH genes, supporting similar genetic identity. CNAG_05113 was sequence and determined to be 45% ID to human TMABADH and 46.2% ID to *Candida albicans* TMABADH using sequence analysis tools services from the EMBL-EBI in 2022[13].

If our hypothesis was true, we predicted that the reintroduction of both carnitine and γBB should restore growth. For the first rescue experiment, I used the Biotek LogPhase Continuous Microplate Reader to generate growth curves. Prior to rescue, I determined that 250 cells/µL was the best concentration for each well (**Figure 8).** I then performed a rescue experiment comparing wild type growth, mutant growth, mutant + 200 µM carnitine, and mutant + 2 mM carnitine concentration at 250 cells/µL in each well. Results of this experiment indicate that full rescue was achieved when carnitine was reintroduced to the mutant cells (**Figure 9).** However, there were difficulties using the LogPhase machine as unpredictable spiking of growth was sometimes observed, likely due to machine error that previous lab members had struggled with. When I repeated the experiment with BBOX **(Figure 10)** as a negative control, having been shown in the lab already to have no growth in acetate, my wild-type concentration spiked at the end in an unpredictable way and there wasn't a clear rescue of my mutant.

I switched to plating rescue experiments using spot assay to visualize the phenotype in hopes that results would be clearer. The results of the spot assay rescue experiments were positive, indicating that rescue was fully successful to restore growth equal to the wild type when carnitine and γBB were present in both 30 ℃ and 37 ℃ conditions **(Figure 11, Figure 12)**. This data supports the hypothesis that CNAG_05113 is involved in the carnitine pathway.

To retry growth curves, I switched to using a shaker in the incubator and taking manual microplate readings in 24-hour increments for 24, 48, and 72 hour timestamps using the Gen5 microplate reading software at 600 nm optical density. This experiment had greater success with more consistent data that indicated restored growth like the spot assay results (**Figure 13, Figure 14)**. I repeated this experiment twice and combined the unique experiments into bar charts with error bars which followed similar trends to the spot assays (**Figure 17, Figure 19).**

The glucose control for the carnitine rescue experiment generated unexpected data, and this experiment should ideally be repeated as the results were inconsistent with the acetate growth

curves and the spot assay plates (**Figure 18**). It was unusual to see mutant growth inhibited on glucose when carnitine was present. However, the glucose control for the γBB rescue experiment was consistent with previous results, as growth is identical for both the mutant and wild type on glucose, with increased growth when γBB is added (**Figure 20)**.

We predicted that virulence factors in our mutant would be affected by the gene deficiency as a defect in acetate metabolism would cause cellular stress that would likely take away cellular energy from virulence pathways. As predicted, there appears to be a defect in mutant melanin production in the 37 °C stressful environment, but not in 30 °C (**Figure 15)**. No apparent difference was observed in capsule production of the mutant compared to the wildtype, but this should be quantified in future research (**Figure 16)**.

Final data analysis of growth curves using 1 and 2 tailed t-test indicated that data was variable, as an ideal T-test value is <0.05. This is likely due to low n value, as the experiment was only repeated twice with 4 duplicates, creating 8 data points for the 48-hour time stamp. This experiment should be repeated in larger quantities to generate better T-test values with lower variance from the mean (**Table 1, Table 2).**

Future directions of this experiment are to identify the genes involved in steps 1, 2, and 4 in the carnitine biosynthesis pathway of *C. neoformans*. Lab members have already been working to identify the first and fourth steps with hypothesized genes responsible that have shown restored growth of mutants in rescue experiments. Eventually, the goal for this project is to generate a therapy that targets the CNAG_05113 gene in *C. neoformans* or another gene involved in the carnitine biosynthesis pathway as a mechanism to kill *C. neoformans* cells in the host. Ideally, an orally administered drug with global accessibility that will not affect the host carnitine pathway.

Acknowledgements

I would like to thank my mentor, Dr. Kerry Smith, for his guidance and support in and outside of the lab. I would also like to thank Rodrigo Catalan-Hurtado and Perry Kezh for their patience in teaching me many protocols and procedures in the lab and directing me through my project. I would like to thank the rest of the Smith Lab and all the EPIC members who have supported me.

I would also like to thank the Creative Inquiry program and the Clemson Honors College for their support and funding for my project through F2022 and S2023 research grants.

References

1. Pescador Ruschel , M. A., & Thapa, B. (2023). Cryptococcal Meningitis . In *Statpearls*. essay, StatPearls Publishing LLC.

2. CDC. (n.d.). *Cryptococcal Screening: A New Strategy for saving lives among people with HIV/AIDS*. Cryptococcal Death Prevention Program. Retrieved May 1, 2023, from https://www.cdc.gov/fungal/pdf/crypto-screen-strategy-508c.pdf

3. Kwon-Chung, K. J., Fraser, J. A., Doering, T. L., Wang, Z. A., Janbon, G., Idnurm, A., & Bahn, Y.-S. (2014). Cryptococcus neoformans and Cryptococcus gattii, the etiologic agents of cryptococcosis. *Cold Spring Harbor Perspectives in Medicine*, *4*(7). https://doi.org/10.1101/cshperspect.a019760

4. May, R. C., Stone, N. R. H., Wiesner, D. L., Bicanic, T., & Nielsen, K. (2015). Cryptococcus: From environmental saprophyte to global pathogen. *Nature Reviews Microbiology*, *14*(2), 106–117. https://doi.org/10.1038/nrmicro.2015.6

5. Tu, A., & Byard, R. W. (2021). Cryptococcosis and unexpected death. *Forensic Science, Medicine and Pathology*, *17*(4), 742–745. https://doi.org/10.1007/s12024-021-00400-1

6. Kharsany, A. B. M., & Karim, Q. A. (2016). HIV infection and AIDS in Sub-Saharan africa: Current status, challenges and opportunities. *The Open AIDS Journal*, *10*(1), 34–48. https://doi.org/10.2174/1874613601610010034

7. Buchanan, K. (1998). What makes Cryptococcus neoformans a pathogen? *Emerging Infectious Diseases*, *4*(1), 71–83. https://doi.org/10.3201/eid0401.980109

8. Ries, L. N., Beattie, S., Cramer, R. A., & Goldman, G. H. (2017). Overview of carbon and nitrogen catabolite metabolism in the virulence of human pathogenic fungi. *Molecular Microbiology*, *107*(3), 277–297. https://doi.org/10.1111/mmi.13887

9. Ferrareze, P. A., Streit, R. S., Santos, P. R., Santos, F. M., Almeida, R. M., Schrank, A., Kmetzsch, L., Vainstein, M. H., & Staats, C. C. (2017). Transcriptional analysis allows genome reannotation and reveals that Cryptococcus gattii VGII undergoes nutrient restriction during infection. *Microorganisms*, *5*(3), 49. https://doi.org/10.3390/microorganisms5030049

10. Strijbis, K., Van Roermund, C. W., Hardy, G. P., Van den Burg, J., Bloem, K., Haan, J., Van Vlies, N., Wanders, R. J., Vaz, F. M., & Distel, B. (2009). Identification and characterization of a complete carnitine biosynthesis pathway in *candida albicans*. *The FASEB Journal*, *23*(8), 2349–2359. https://doi.org/10.1096/fj.08-127985

11. Kugler, P., Trumm, M., Frese, M., & Wendisch, V. F. (2021). L-carnitine production through biosensor-guided construction of the neurospora crassa biosynthesis pathway in escherichia coli. *Frontiers in Bioengineering and Biotechnology*, *9*. https://doi.org/10.3389/fbioe.2021.671321

12. http://busca.biocomp.unibo.it/deepmito/

13. https://www.ebi.ac.uk/Tools/psa/emboss_needle

Tables and Figures

Table 1. Carnitine T-test Results for 48 hr

	Average	1 Tail T-test mutant	2 Tailed T-test mutant	Standard Deviation	Standard Error
K99 wild type	0.211875	0.113084443	0.226168887	0.035850633	0.010809372
ALD13 mutant	0.19375	**1 Tail T-test mutant + C**	**2 Tailed T-test mutant + C**	0.017202575	0.005734192
ALD13 + 200 uM C	0.21825	0.328716444	0.657432889	0.016420806	0.004951059

Table 2. Gamma-butyrobetaine T-test results for 48 hr

	Average	1 Tail T-test mutant	2 Tailed T-test mutant	Standard Deviation	Standard Error
K99 wild type	0.19825	0.081969486	0.163938971	0.027845236	0.008038227
ALD13 mutant	0.18175	**1 Tail T-test mutant + γBB**	**2 Tailed T-test mutant + γBB**	0.013936079	0.004406975
ALD13 + 200 uM γBB	0.199375	0.461323571	0.922647143	0.015837907	0.005008386

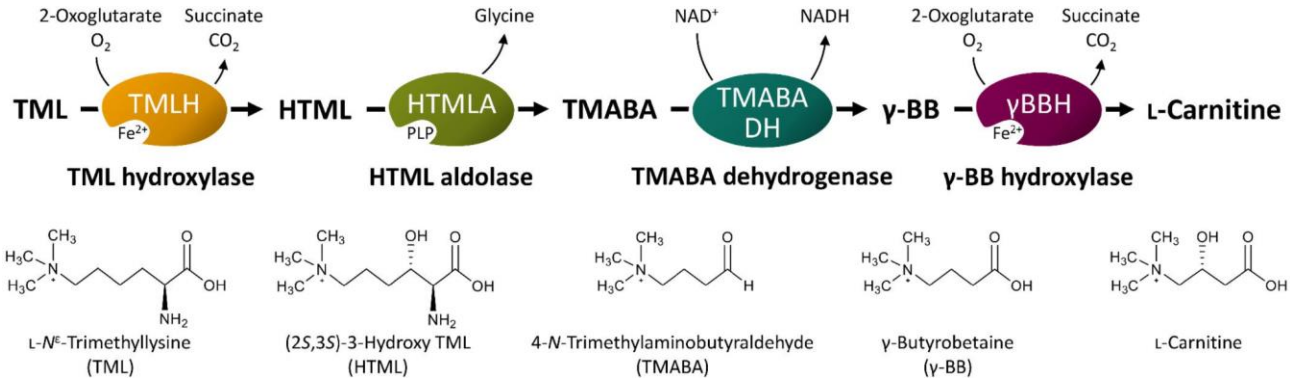

Figure 1. Carnitine Biosynthetic Pathway via Kugler et al[10].

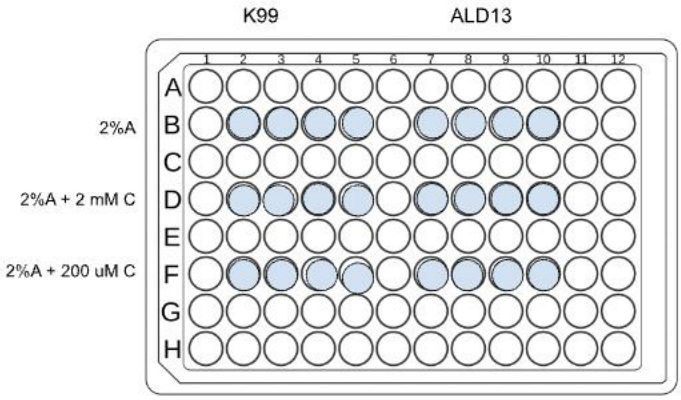

Figure 2. Visual of LogPhase growth curve plating set-up. Performed 4 replicates of each condition, plating both the wild type and ALD13 mutant in 2%A media with variable carnitine concentrations- no carnitine, 2 mM carnitine, and 200 µM carnitine concentration.

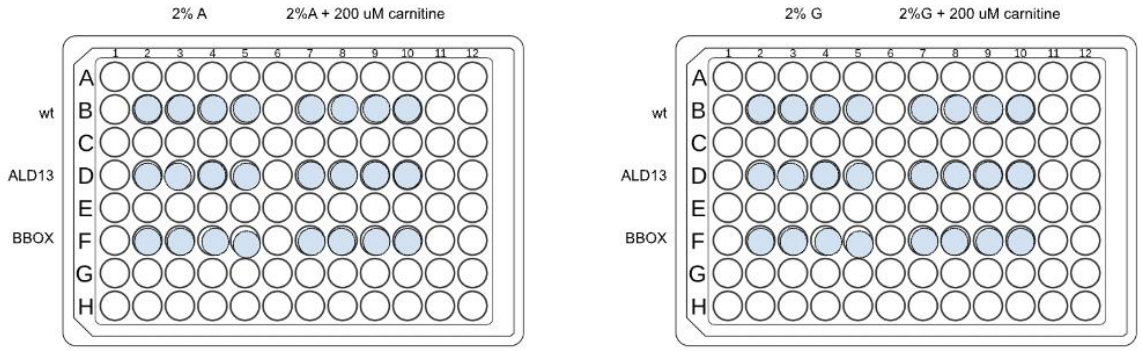

Figure 3. Visual of LogPhase carnitine rescue growth curve plate setup for repeat experiment with BBOX mutant and only 200 µM carnitine concentration.

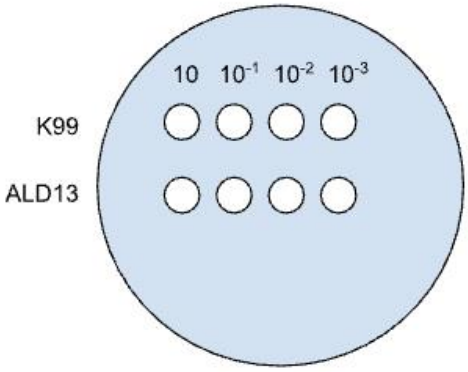

Figure 4. Visual of spot assay dilution used for gamma-butyrobetaine and carnitine rescue plating experiments.

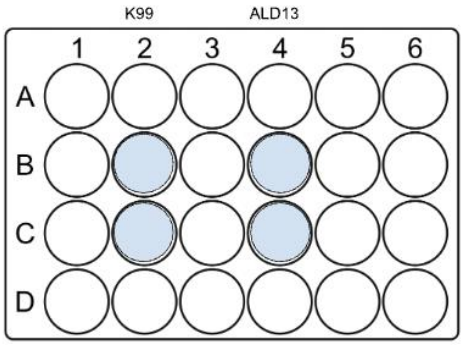

Figure 5. Visual of plate set up for capsule experiment using a 24 well plate and duplicates of both strains grown in DMEM + 10% fetal bovine serum.

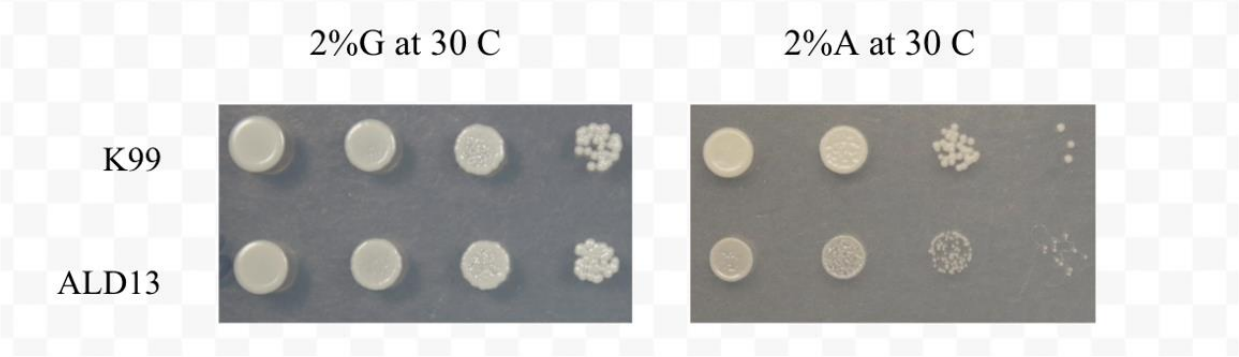

Figure 6. Wild type and ALD13 mutant plated on glucose and acetate carbon sources showed defective growth of the mutant on acetate compared to glucose at 30°C.

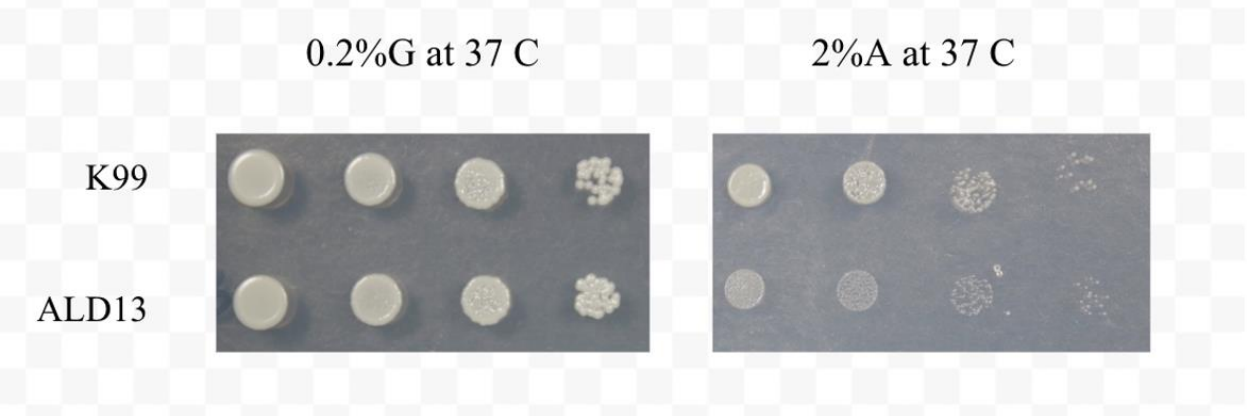

Figure 7. Wild type and ALD13 mutant plated on glucose and acetate carbon sources showed defective growth of the mutant on acetate compared to glucose at 37°C.

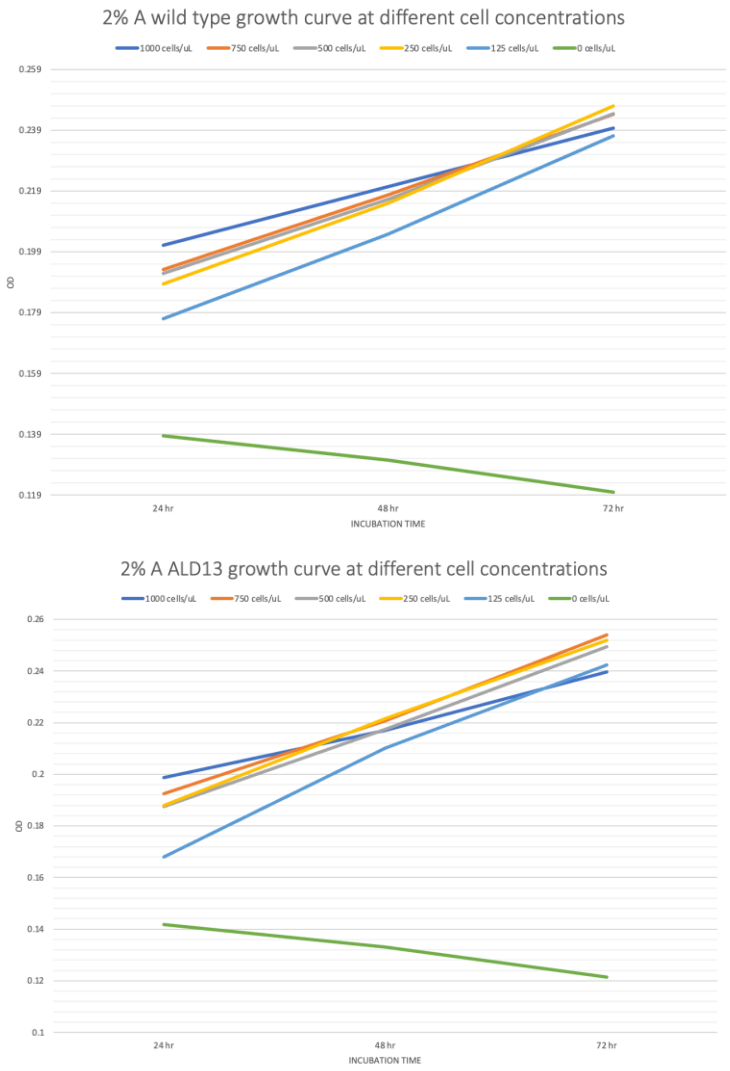

Figure 8. Graphical representation of growth curve of wild type and mutant in 2%A at variable cell concentrations. Used to determine the best concentration for future experimentation. In both strains, 250 cells/uL had the best concentration results in 200 uL well size over a 72 hour time period, so I moved forward with this concentration for all other growth curve experiments. Incubated at 37 ℃ and timestamps taken every 5 minutes, captured by the BioTek LogPhase at 600 nm optical density.

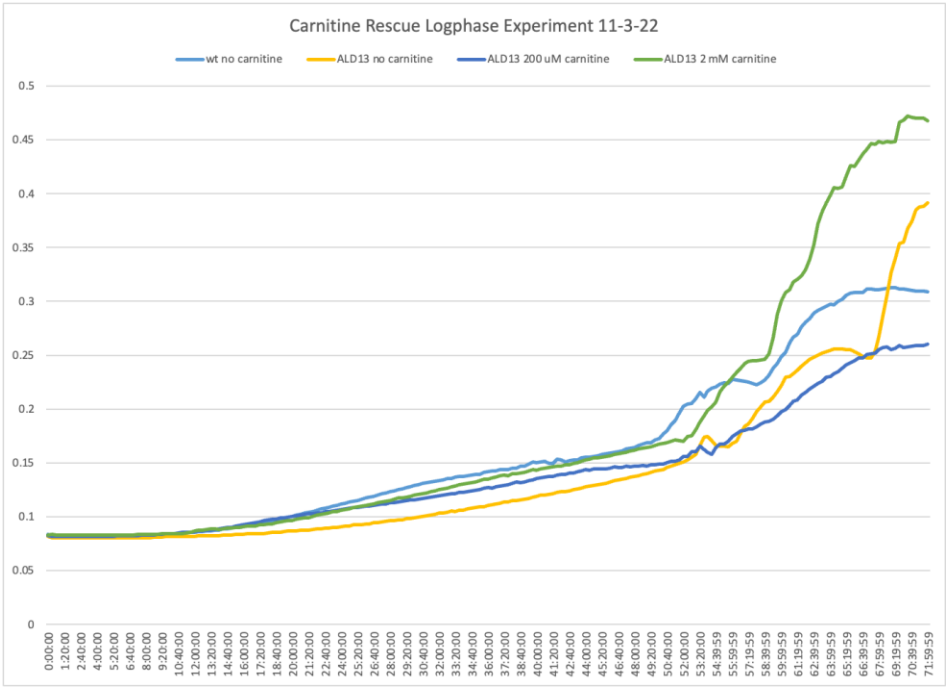

Figure 9. Carnitine rescue experiment in the Log Phase cell counter. These results indicated defective growth of the mutant in 2%A without carnitine, and restored growth in 2%A + 200 uM and 2 mM concentrations of carnitine to match the wild type.

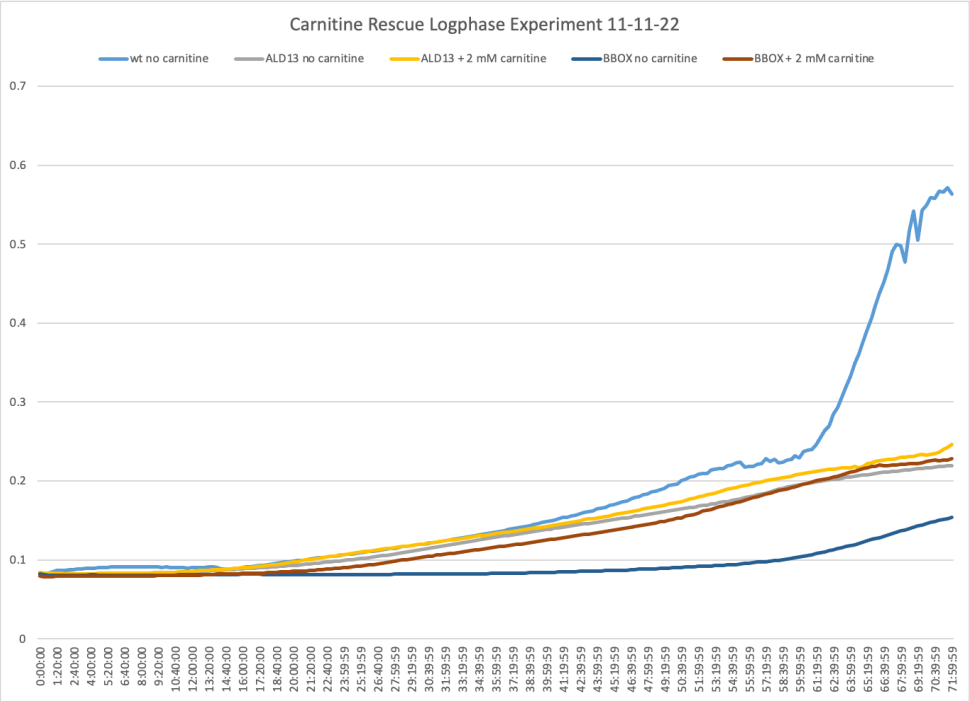

Figure 10. Carnitine rescue experiment in the LogPhase cell counter with BBOX as a negative control.

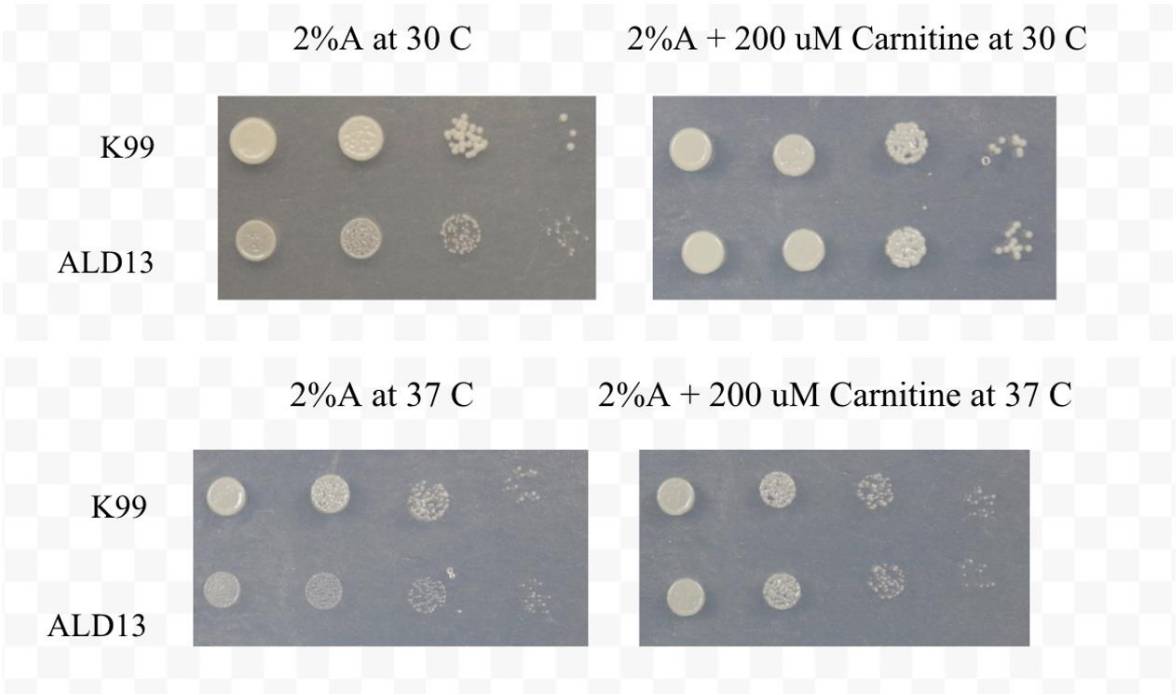

Figure 11. Carnitine rescue experiment performed on acetate plates with 200 uM carnitine concentration and acetate control at both 30 C and 37 C. Found full rescue of ALD13 cells in both temperature conditions in the presence of carnitine.

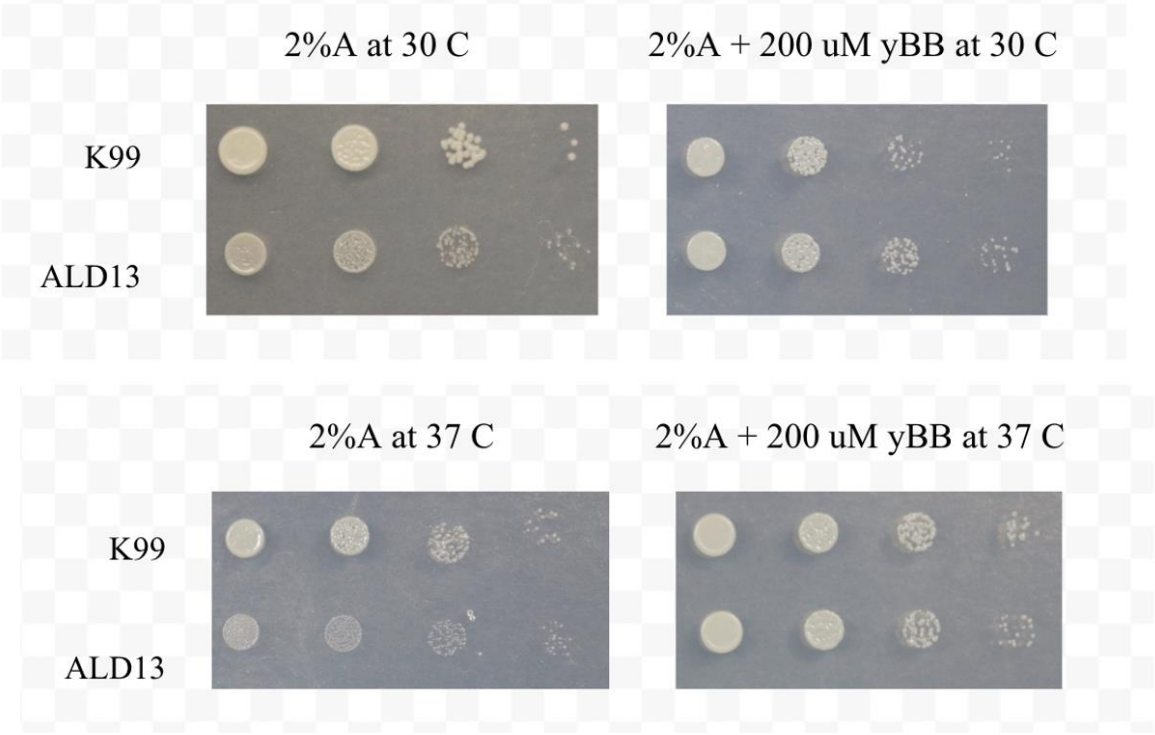

Figure 12. γBB rescue experiment performed on acetate plates with 200 uM γBB concentration at both 30°C and 37°C. Full rescue observed of mutant cells in both temperature conditions when 200 uM γBB is present.

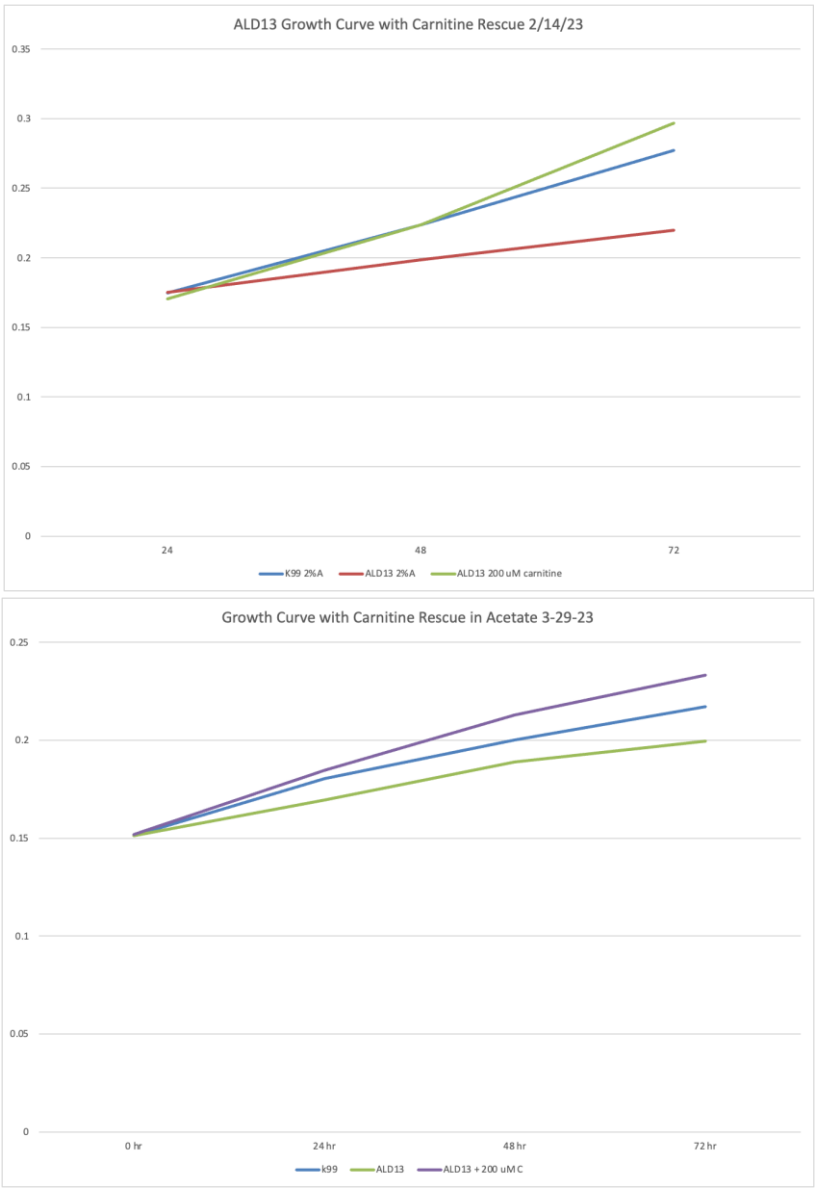

Figure 13. Carnitine rescue experiment growth curves in acetate. Incubated at 30 ℃ and time stamps taken with Gen5 Microplate Reading Software at 600 nm Absorbance Optical Density every 24 hours from 24-72 hr.

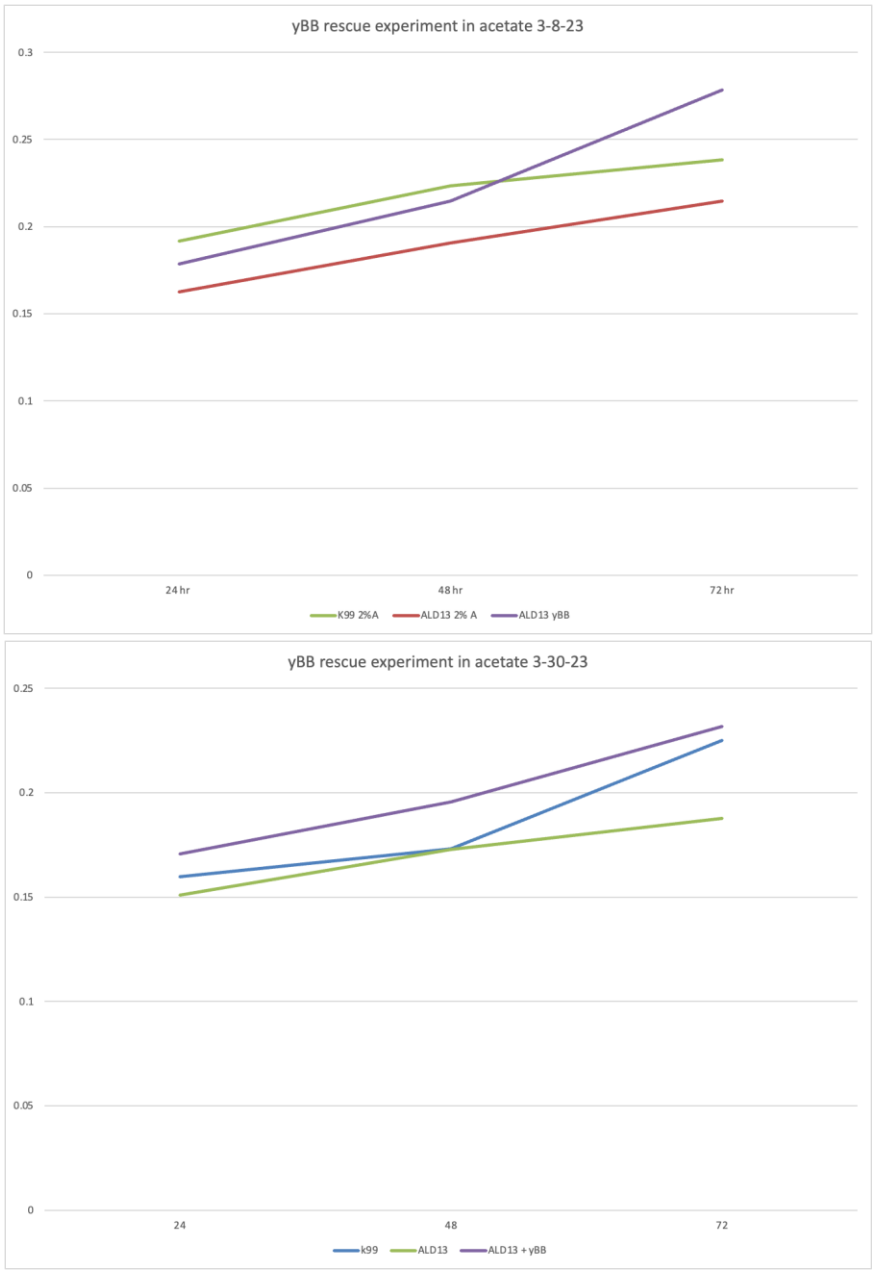

Figure 14. γBB rescue experiment growth curves in acetate. Carnitine rescue experiment growth curves in acetate. Incubated at 30 ℃ and time stamps taken with Gen5 Microplate Reading Software at 600 nm Absorbance Optical Density every 24 hours from 24-72 hr.

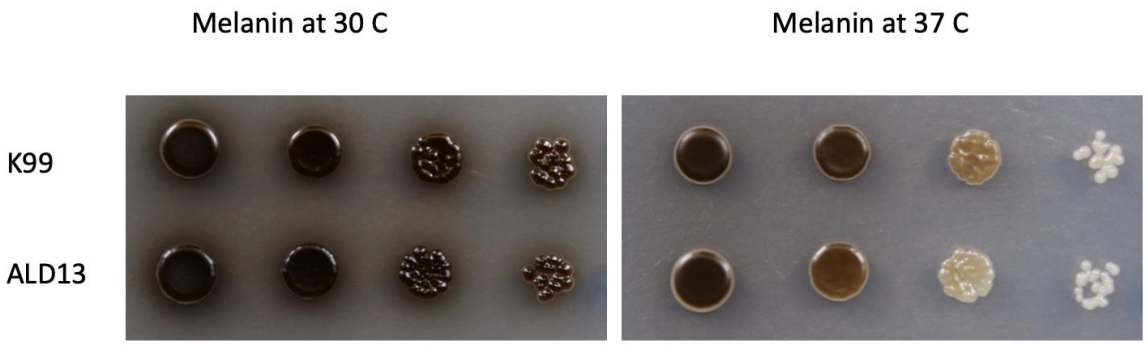

Figure 15. Wild type and mutant cells were grown on melanin plates for 48-72 hours in both 30°C and 37°C incubators.

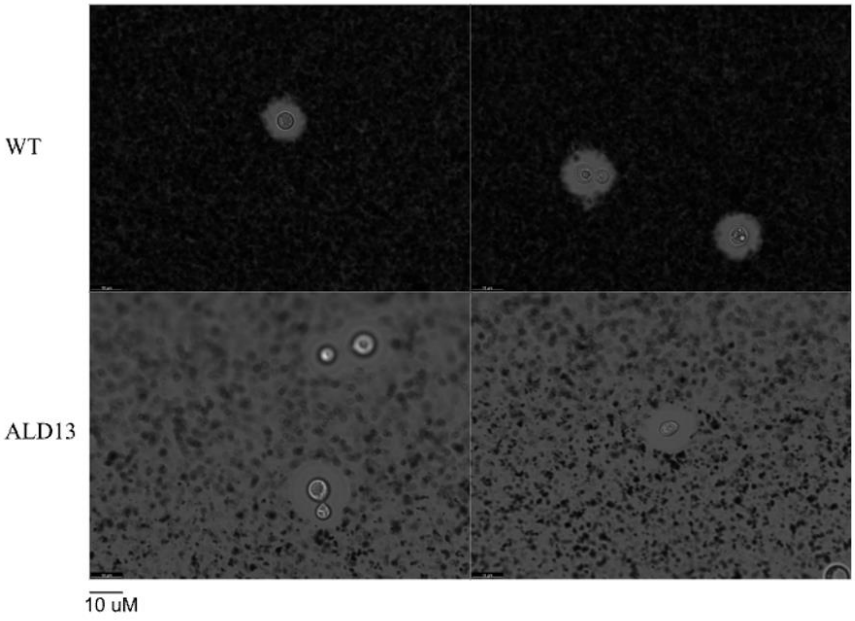

Figure 16. Capsule images taken of both wild type and mutant stained with India ink in the Leica microscope.

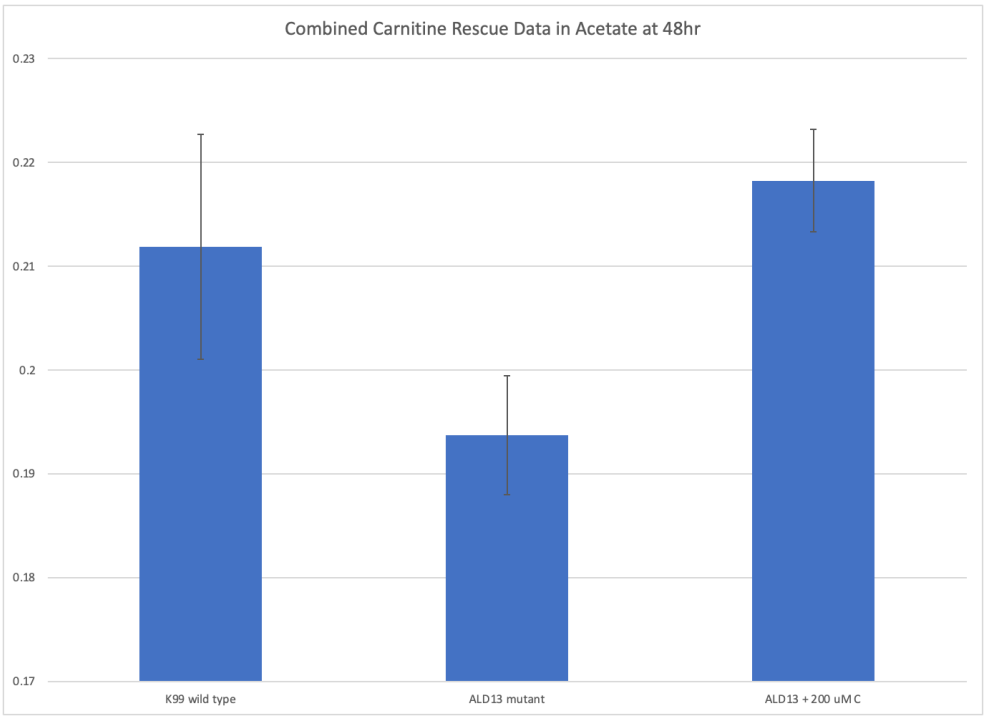

Figure 17. Carnitine rescue experiment in acetate bar chart. Using combined data from two unique carnitine rescue experiments at 48hr timestamps, including error bars calculated from standard error.

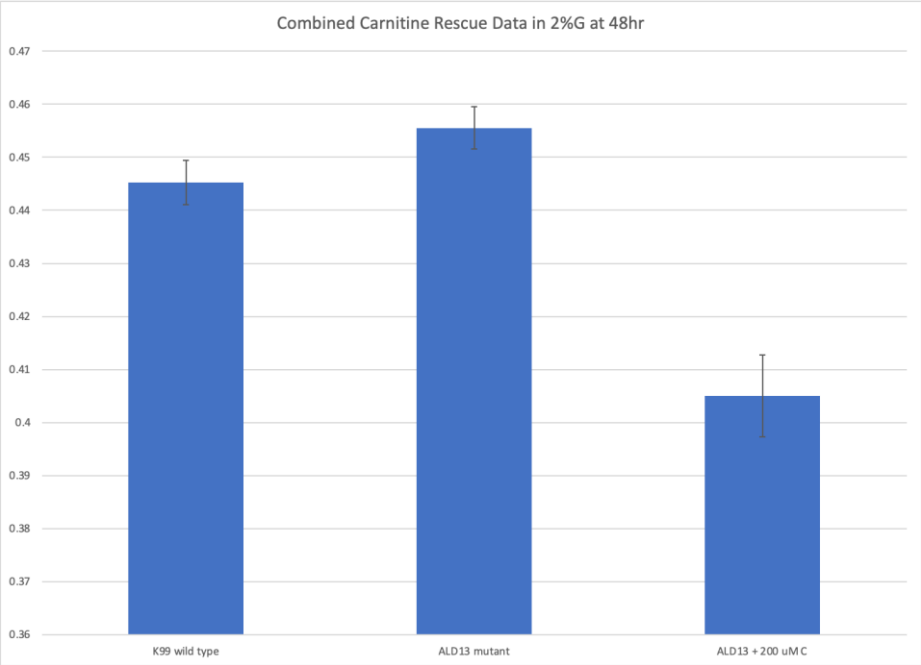

Figure 18. Carnitine rescue experiment in glucose bar chart. Using combined data from two unique carnitine rescue experiments at 48hr timestamps, including error bars calculated from standard error.

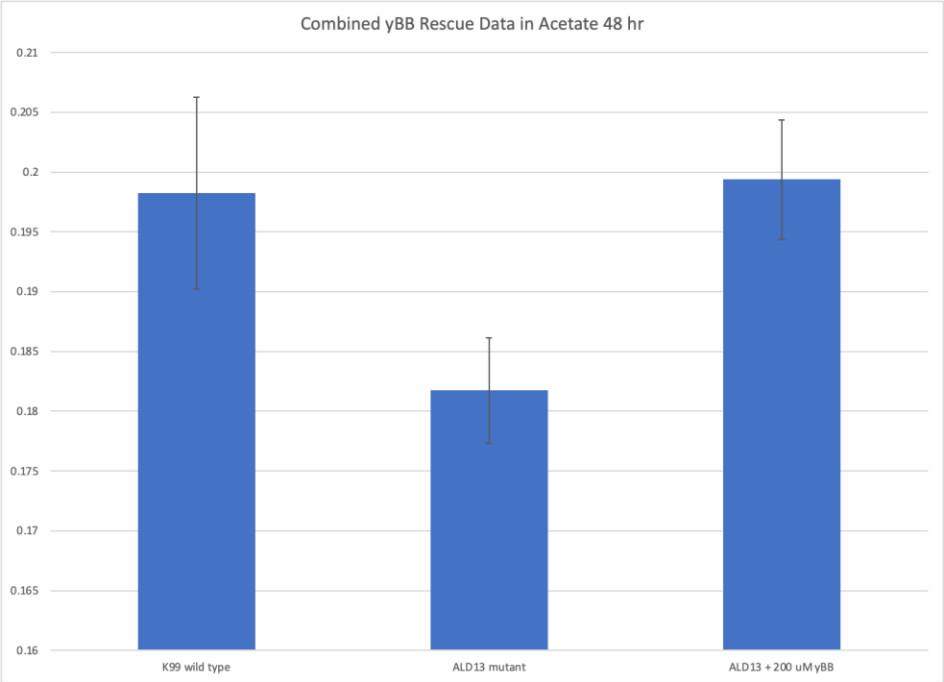

Figure 19. γBB rescue experiment bar chart in acetate. Using combined data from two unique carnitine rescue experiments at 48hr timestamps, including error bars calculated from standard error.

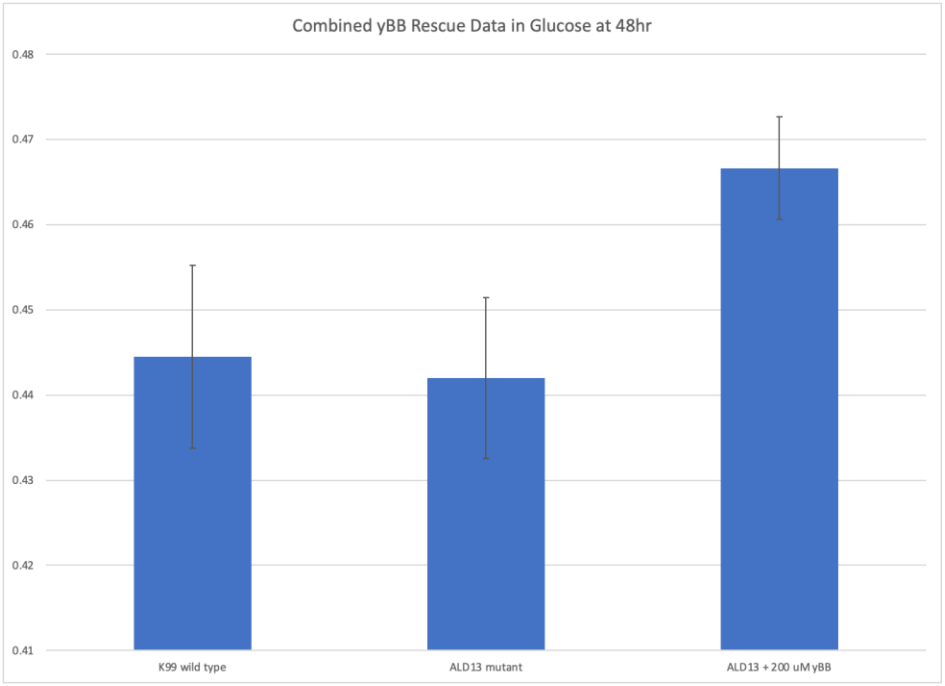

Figure 20. γBB rescue experiment bar chart in glucose. Using combined data from two unique carnitine rescue experiments at 48hr timestamps, including error bars calculated from standard error.